High-Frequency and Field EPR Investigation of (8,12-Diethyl-2,3,7,13,17,18-hexamethylcorrolato)manganese(III)

J. Krzystek,*,† Joshua Telser,‡ Brian M. Hoffman,§ Louis-Claude Brunel,† and Silvia Licoccia⊥

Contribution from the Center for Interdisciplinary Magnetic Resonance, National High Magnetic Field Laboratory, Florida State University, Tallahassee, Florida 32310, Chemistry Program, Roosevelt University, Chicago, Illinois 60605, Department of Chemistry, Northwestern University, Evanston, Illinois 60208, and Dipartimento di Scienze e Tecnologie Chimiche, Università di Roma Tor Vergata, 00133 Rome, Italy

Received April 12, 2001. Revised Manuscript Received June 7, 2001

Abstract: High-field and frequency electron paramagnetic resonance (HFEPR) of solid (8,12-diethyl-2,3,7,13,17,18-hexamethylcorrolato)manganese(III), **1**, shows that in the solid state it is well described as an $S = 2$ (high-spin) Mn(III) complex of a trianionic ligand, $[Mn^{III}C^{3-}]$, just as Mn(III) porphyrins are described as $[Mn^{III}P^{2-}]^{+}$. Comparison among the structural data and spin Hamiltonian parameters reported for **1**, Mn(III) porphyrins, and a different Mn(III) corrole, [(tpfc)Mn(OPPh$_3$)], previously studied by HFEPR (Bendix, J.; Gray, H. B.; Golubkov, G.; Gross, Z. *J. Chem. Soc., Chem. Commun*. **2000**, 1957−1958), shows that despite the molecular asymmetry of the corrole macrocycle, the electronic structure of the Mn(III) ion is roughly axial. However, in corroles, the $S = 1$ (intermediate-spin) state is much lower in energy than in porphyrins, regardless of axial ligand. HFEPR of **1** measured at 4.2 K in pyridine solution shows that the $S = 2$ $[Mn^{III}C^{3-}]$ system is maintained, with slight changes in electronic parameters that are likely the consequence of axial pyridine ligand coordination. The present result is the first example of the detection by HFEPR of a Mn(III) complex *in solution*. Over a period of hours in pyridine solution at ambient temperature, however, the $S = 2$ Mn(III) spectrum gradually disappears leaving a signal with $g = 2$ and ^{55}Mn hyperfine splitting. Analysis of this signal, also observable by conventional EPR, leads to its assignment to a manganese species that could arise from decomposition of the original complex. The low-temperature $S = 2$ $[Mn^{III}C^{3-}]$ state is in contrast to that at room temperature, which is described as a $S = 1$ system deriving from antiferromagnetic coupling between an $S = {}^3/_2$ Mn(II) ion and a corrole-centered radical cation: $[Mn^{II}C^{\bullet 2-}]$ (Licoccia, S.; Morgante, E.; Paolesse, R.; Polizio, F.; Senge, M. O.; Tondello, E.; Boschi, T. *Inorg. Chem.* **1997**, *36*, 1564−1570). This temperature-dependent valence state isomerization has been observed for other metallotetrapyrroles.

Introduction

Among the numerous cyclic tetrapyrroles that are known, the corrole has attracted significant interest due to its structure, which is intermediate between that of a porphyrin and that of a corrin.[1,2] The 18-electron aromatic π system of corroles is identical with that of porphyrins, but there is a direct link between two of the pyrrole rings, as found in corrins (Chart 1). Furthermore, porphyrins have two amino donor atoms, and are thus dianionic ligands, while corroles have three amino nitrogens and thus behave as trianionic ligands. This more negative ligand charge may stabilize higher oxidation states of coordinated transition metal ions,[2−4] which may be the reason that transition metal corroles have shown promise as oxidation catalysts,[5] a role for which metalloporphyrins have already been widely used.[6] Studies on the applications of metal complexes of tetrapyrroles have been complemented by spectroscopic methods, such as NMR and EPR. EPR is particularly useful in investigating the paramagnetic metal center in these complexes, even when large axial zero-field splitting (zfs) in non-Kramers (integer spin) systems makes a complex "EPR-silent" in the solid state at X-band, such as is often found for Mn(III) ($3d^4$, $S = 2$). High-frequency and field EPR (HFEPR) is especially effective at detecting resonances from Mn(III).[7−11] These

Chart 1

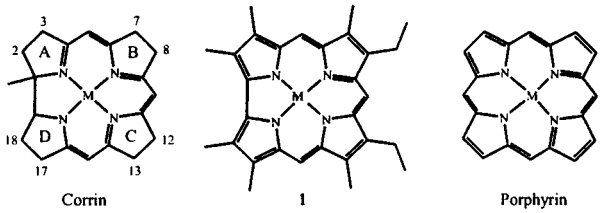

† Florida State University.
‡ Roosevelt University.
§ Northwestern University.
⊥ Università di Roma Tor Vergata.

(1) Licoccia, S.; Paolesse, R. *Struct. Bonding* **1995**, *84*, 73−133.
(2) Kadish, K. M.; Adamian, V. A.; van Caemelbecke, E.; Gueletii, E.; Will, S.; Erben, C.; Vogel, E. *J. Am. Chem. Soc.* **1998**, *120*, 11986−11993.
(3) Meier-Callahan, A. E.; Gray, H. B.; Gross, Z. *Inorg. Chem*. **2000**, *39*, 3605−360
(4) Walker, F. A. *The Porphyrin Handbook*; Academic Press: San Diego, 2000; Vol. 5, Chapter 36, pp 81−184.
(5) Gross, Z.; Simkhovich, L.; Galili, N. *J. Chem. Soc., Chem. Commun.* **1999**, 599−600.
(6) Sheldon, R. A., Ed. *Metalloporphyrins in Catalytic Oxidations*; Marcel Dekker: New York, 1994.
(7) Goldberg, D. P.; Telser, J.; Krzystek, J.; Montalban, A. G.; Brunel, L. C.; Barrett, A. G. M.; Hoffman, B. M. *J. Am. Chem. Soc.* **1997**, *119*, 8722−8723.

10.1021/ja010947g CCC: $20.00 © 2001 American Chemical Society
Published on Web 07/21/2001

HFEPR studies have unequivocally confirmed the spin state ($S = 2$) and formal oxidation state (3+) of the manganese ion in solid complexes of porphyrins[7,8] and, very recently, of a corrole, [(tpfc)Mn($OPPh_3$)] (tpfc = 5,10,15-tris(pentafluorophenyl)-corrole trianion), as well.[10] Thus the solid complexes can best be represented as $[Mn^{III}P^{2-}]^+$ and $[Mn^{III}C^{3-}]$ for porphyrins and corroles, respectively.

Previous studies on porphyrins[12] and on corroles in solution,[1,13,14] however, suggest variation in the spin and oxidation state of the manganese ion when in the presence of axial ligands. In particular, NMR experiments as reported by Turner and Gunter[12] strongly suggested $[MnTPP]^+$ (TPP = 5,10,15,20-tetraphenylporphyrin dianion) in solution as being best described as $[Mn^{II}P^{\bullet-}]^+$. The total spin is still $S_{total} = 2$, but would result instead from an intermediate spin ($S = {}^3/_2$) Mn(II) ferromagnetically coupled to a $S = {}^1/_2$ radical ion created on the porphyrin ring. Similarly, both solution NMR and magnetic susceptibility studies, all at ambient temperature, of manganese β-alkylcorrolates in coordinating solvents indicated the existence of an analogous valence state isomerism induced by intramolecular ligand-to-metal electron transfer, thus suggesting the formulation of the complexes as $[Mn^{II}C^{\bullet 2-}]$, in analogy to MnTPP.[13] The proton NMR spectra of manganese corroles show resonances spread over a wide spectral region with very positive chemical shifts of the *meso*-H signals, characteristic of a macrocycle centered radical.[4] We have therefore performed HFEPR experiments on a Mn(III) corrole, (8,12-diethyl-2,3,7,13,17,18-hexamethylcorrolato)manganese(III), **1** (Chart 1), to confirm the $S = 2$ spin state of the complex in the solid state and investigate its electronic structure in comparison to related complexes. We also describe HFEPR studies of **1** in frozen solution to shed more light on the electronic structure of **1** under those conditions.

Experimental Section

Complex **1** was synthesized and checked for purity as described previously.[13] For HFEPR experiments, the polycrystalline sample obtained from the final recrystallization was first used "as is" i.e., in a loose form. The material was subsequently divided into two batches to apply each of two methods for ensuring a powder pattern distribution by preventing crystallite reorientation (torquing) in the high magnetic fields. One batch was ground with KBr and pressed into a pellet and the other batch was mixed with molten eicosane and allowed to solidify. The typical amount of solid complex **1** in all experiments was between 15 and 20 mg. For the frozen solution experiment, the eicosane from the second batch was extracted with pentane (Sigma, analytical grade), which was consequently evaporated, and complex **1** was dissolved in pyridine (Sigma, spectroscopic grade) at a nominal concentration of 0.2 M. The typical volume of solution used in the experiment was 200 μL. Pyridine was previously thoroughly purged of oxygen using dry nitrogen gas flow to minimize the intensity of solid oxygen lines appearing in the low-temperature spectra.[15] HFEPR spectra were recorded in a 95−575 GHz frequency range using the locally constructed transmission-type multifrequency instrument.[16] The instrument settings are contained in the figure captions. X-band and Q-band (35 GHz) EPR spectra were recorded, respectively, at 77 K on a modified Varian E-9 spectrometer and at 4.2 K on a locally constructed pulsed spectrometer, which allows electron spin−echo detected EPR spectra to be collected.[17]

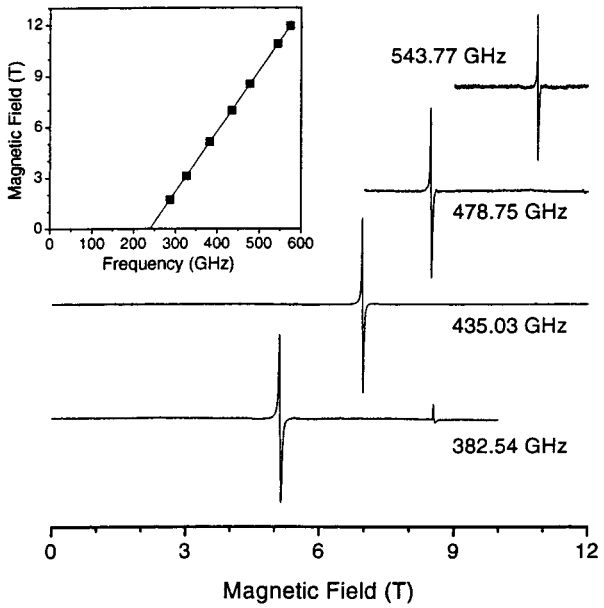

Figure 1. Representative HFEPR spectra at 4.2 K of solid loose complex **1** at different frequencies. The spectra were normalized to approximately equal amplitude, and the phase was corrected by software to account for dispersive components. The weak signal visible above the dominant one at 382.5 GHz originates from a higher harmonic generated by the source. Instrumental settings: field sweep rate, 0.2 T/min; field modulation, 8 kHz frequency, 1.5 mT amplitude; time constant, 0.3 s; applied mm or sub-mm power strongly varied with frequency. Inset: Resonance field vs frequency dependence of the same transition. The squares represent experimental points while the line was drawn assuming that the observed signal corresponds to the parallel $|S, M_S\rangle = |2, -2\rangle \rightarrow |2, -1\rangle$ transition of the $S = 2$ spin manifold, using best-fit spin Hamiltonian parameters: $D = -2.66$ cm^{-1}, $E = 0$, isotropic $g = 2.00$.

Results

Solid Loose Sample. The EPR spectrum of solid loose complex **1** is dominated by a single line observed at all frequencies >220 GHz and at temperatures ≤20 K, as shown in Figure 1 for several frequencies. The resonant field increases linearly with increasing frequency (Figure 1, inset). Since this behavior is very characteristic for the $S = 2$ spin state of field-oriented solid Mn(III) porphyrins, we followed the procedure established previously[7,8] to extract spin Hamiltonian parameters as defined by:

$$\mathbf{H} = \beta B \cdot \mathbf{g} \cdot S + D(S_z^2 - S(S+1)/3) + E(S_x^2 - S_y^2) \quad (1)$$

The observed signal is assigned to the $|S, M_S\rangle = |2, -2\rangle \rightarrow |2, -1\rangle$ parallel transition, as is the case for other $S = 2$ systems with negative D,[7,8] based on simulation of the magnetic resonance field versus quantum energy dependence as shown in Figure 2. The lack of corresponding perpendicular transitions proves that the external magnetic field aligns the microcrystal-

(8) Krzystek, J.; Telser, J.; Pardi, L. A.; Goldberg, D. P.; Hoffman, B. M.; Brunel, L. C. *Inorg. Chem.* **1999**, *38*, 6121−6129.
(9) Barra, A.-L.; Gatteschi, D.; Sessoli, R.; Abbati, G. L.; Cornia, A.; Fabretti, A. C.; Uytterhoeven, M. G. *Angew. Chem., Int. Ed. Engl.* **1997**, *36*, 2329−2331.
(10) Bendix, J.; Gray, H. B.; Golubkov, G.; Gross, Z. *J. Chem. Soc., Chem. Commun.* **2000**, 1957−1958.
(11) Limburg, J.; Vrettos, J. S.; Crabtree, R. H.; Brudvig, G. W.; de Paula, J. C.; Hassan, A.; Barra, A.-L.; Duboc-Toia, C.; Collomb, M.-N. *Inorg. Chem.* **2001**, *40*, 1698−1703.
(12) Turner, P.; Gunter, M. J. *Inorg. Chem.* **1994**, *33*, 1406−1415.
(13) Licoccia, S.; Morgante, E.; Paolesse, R.; Polizio, F.; Senge, M. O.; Tondello, E.; Boschi, T. *Inorg. Chem.* **1997**, *36*, 1564−1570.
(14) Erben, C.; Will, S.; Kadish, K. M. *The Porphyrin Handbook*; Academic Press: San Diego, 2000; Vol. 2, Chapter 12, pp 233−300.
(15) Pardi, L. A.; Krzystek, J.; Telser, J.; Brunel, L. C. *J. Magn. Reson.* **2000**, *146*, 375−378.
(16) Hassan, A. K.; Pardi, L. A.; Krzystek, J.; Sienkiewicz, A.; Goy, P.; Rohrer, M.; Brunel, L. C. *J. Magn. Reson.* **2000**, *142*, 300−312.
(17) Davoust, C. E.; Doan, P. E.; Hoffman, B. M. *J. Magn. Reson.* **1996**, *A119*, 38−44.

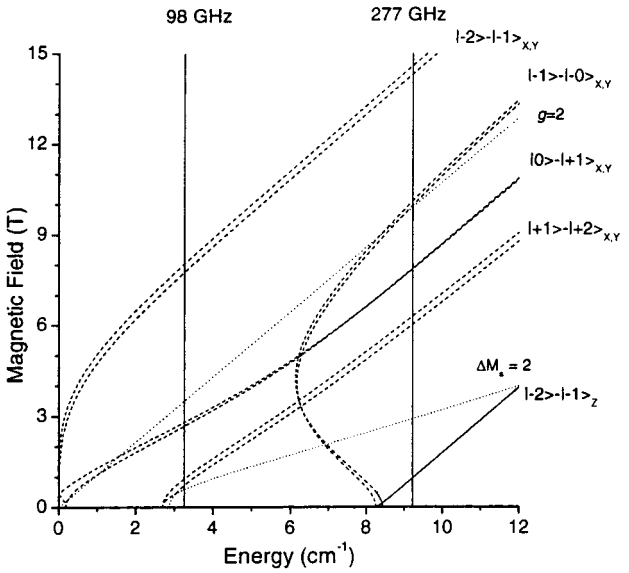

Figure 2. Plot of resonance field vs transition energy of complex **1** in frozen pyridine solution using spin Hamiltonian parameters as in Table 1 (parameters characteristic for the solid produce very similar dependencies). For clarity, only those transition branches are plotted that are observed experimentally in Figures 1, 3, and 5. The solid line is the EPR resonance branch for B_0 along z, the same branch as plotted in Figure 1, and the dashed lines are those for B_0 along x and y orientations. The dotted line is for B_z with $|\Delta M_S| = 2$ (partially allowed transition). The $g = 2$ dependence is also included. The ground state $|M_S\rangle$ to excited state $|M_S\rangle$ levels are indicated, based on a energy level diagram for this system (not shown), with a caveat that the high-field spin functions are in reality mixtures of the zero-field levels. The transition energies are calculated by diagonalizing the spin Hamiltonian matrix. Resonant field vs transition energy (or frequency) plots such as this are very useful in identifying any transitions present in a spectrum at a given frequency. For example, the vertical line at energy corresponding to 98 GHz shows that only perpendicular (and one partly allowed) transitions are expected (as in Figure 5), since all the parallel transitions are out of the frequency range. The 277 GHz spectrum, on the other hand, contains the B_z $|2, -2\rangle \rightarrow |2, -1\rangle$ transition near 1 T, as detected experimentally in Figure 3C.

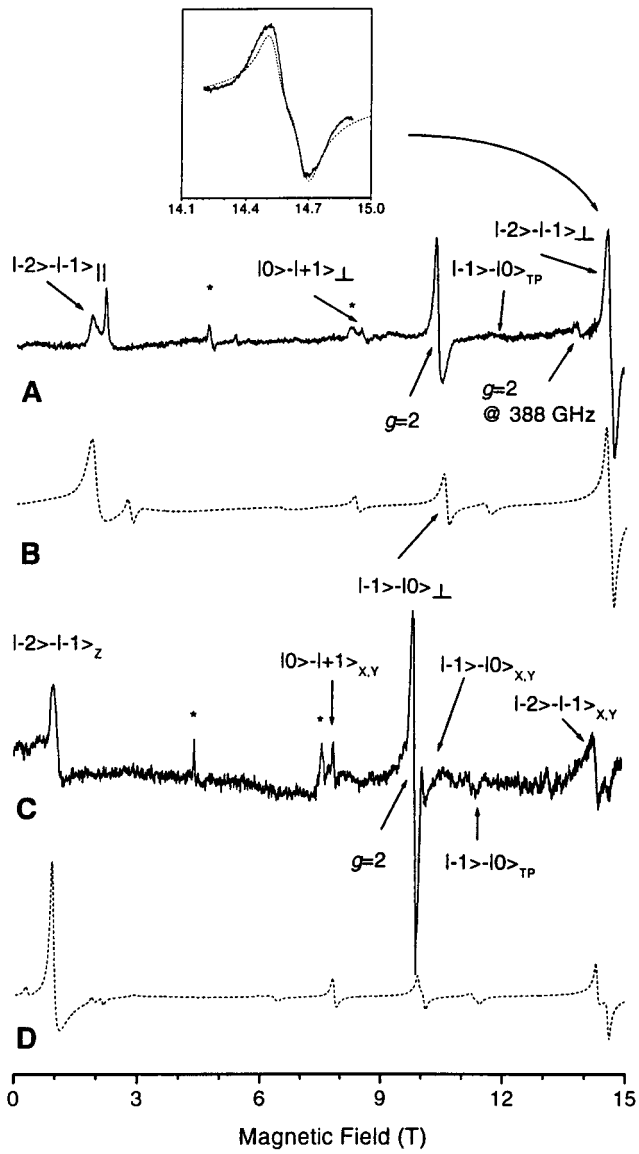

Figure 3. (A) EPR spectrum of complex **1** embedded in eicosane mull at 291.41 GHz and 4.2 K. Experimental conditions as in Figure 1. The particular transitions in the powder pattern are identified and labeled accordingly. "TP" stands for an off-axis turning point. The sharp signal at 2.2 T is discussed in the text. The two lines marked with asterisks originate from solid molecular oxygen present in the sample area. Inset: The perpendicular $|S, M_S\rangle = |2, -2\rangle \rightarrow |2, -1\rangle$ transition on an expanded field scale. The experimentally observed (solid line) doubling of that transition is reproduced in the simulation (broken line) by introducing a rhombic term $E = 0.015$ cm^{-1}. (B) Simulation of spectrum A using spin Hamiltonian parameters given in Table 1. The $g = 2.00$ impurity signal is not reproduced in the simulation. (C) EPR spectrum of a frozen pyridine solution of complex **1**. Frequency 276.62 GHz, $T = 4.2$ K. Experimental conditions as in Figure 1. Since the spectrum shows observable rhombicity of the zfs tensor ($E = 0.03$ cm^{-1}), we used a labeling convention different from the solid spectra (x-, y-, and z-transitions rather than perpendicular and parallel). A shift of the spectrum toward lower frequencies is due to a lower operating frequency than in spectrum A, however, the increased splitting between the z- and x, y-transitions is due to an increase of $|D|$. (D) Simulation of spectrum C using spin Hamiltonian parameters as in Table 1.

lites with their largest anisotropy axis parallel to the field. The field dependence of the transition is strictly linear (Figure 1, inset), which indicates that E must be small ($E/D < 0.05$).[7,8] The slope yields an approximate value of $g_{||} = 2.00$ and the intercept with the frequency axis corresponds to $3|D|$ with $D = -2.66$ cm^{-1}.

It is also possible to detect a weak $g = 2$ signal in the HFEPR spectra at any frequency within the magnet field range (not shown). Its intensity behaves differently with respect to temperature than the previously identified $S = 2$ line: the $S = 2$ signal becomes unobservable at temperatures >20 K, while the $g = 2$ line becomes more pronounced and narrowed with increasing temperature and frequency, so that at 388 GHz and at 20 K and above it reveals a partly resolved hyperfine sextet typical for Mn(II). It should be stressed that the integrated intensity of this Mn(II) signal is much smaller than that of Mn(III) (see below).

Solid Immobilized Sample. The experiment performed on solid, field-oriented **1** does not yield the complete set of spin Hamiltonian parameters. To obtain these parameters, we thus prevented microcrystallite orientation either by pressing a KBr pellet or embedding the sample in an eicosane mull. The HFEPR spectra obtained using both methods are essentially identical. Figure 3A shows a representative eicosane mull spectrum at 291.41 GHz. This spectrum is distinctly different from that of the loose sample. The intensity of the previously dominating line at 1.9 T is greatly reduced and a strong signal appears at 14.6 T that is absent in the loose sample. A straightforward assignment of this signal is to the perpendicular $|2, -2\rangle \rightarrow |2, -1\rangle$ transition that was missing in the field-oriented sample. A

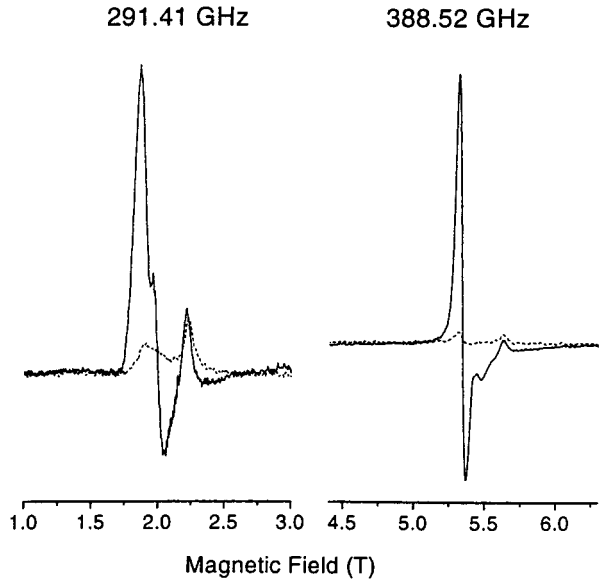

Figure 4. HFEPR spectra of complex **1** as a loose, field-oriented solid (solid lines), and embedded in eicosane mull (broken lines) at two frequencies and $T = 4.2$ K. Experimental conditions as in Figure 1. Exactly the same amount of sample (18 mg) was used in all experiments.

Table 1. Spin Hamiltonian Parameters of Mn(III) Corrole Complexes, Determined by HFEPR

	D (cm^{-1})	E (cm^{-1})	$g_{\|\|}$	$g_\perp$
loose solid **1**	−2.66(2)	<0.13	2.00(2)	
immobilized solid **1**	−2.64(1)	0.015(5)	2.00(1)	2.02(1)
pyridine solution of **1**	−2.78(1)	0.030(5)	2.00(2)	2.00(2)
[(tpfc)Mn(OPPh$_3$)] [a]	−2.69(2)	0.030(3)	1.980(4)	1.994(4)

[a] Work of Bendix et al.,[10] with corrected sign of D.[28]

random distribution of microcrystallites throughout the sample was thus achieved. The $g = 2$ signal persists at 10.4 T without significant intensity change. All of the signals can be relatively easily attributed (see below), with the exception of a signal at 2.2 T.

Comparison of Figures 1 and 3A might suggest that the signal at 2.2 T appeared only after immobilizing the microcrystallites by either method; however, careful inspection of the spectra of the loose sample shows its presence there as well. Figure 4 shows representative spectra of a loose sample (solid line), and the same amount of the immobilized sample (dotted line) at two frequencies. The intensity of the $|2, -2\rangle \rightarrow |2, -1\rangle$ parallel transition is much lower in the powder pattern (immobilized) sample, but the intensity of the "extra" line (2.2 T at 291 GHz and 5.6 T at 389 GHz) remains unchanged. Furthermore, simulation shows that the resonance field vs frequency behavior of the "extra" line does not correspond to any transition of the $S = 2$ manifold. We thus assign it to an unidentified impurity rather than to the spin system of interest.

To obtain the complete set of spin Hamiltonian parameters, we performed spectral simulations using the program described by Jacobsen et al.[18] The numerical results are presented in Table 1 and a simulated spectrum is presented in Figure 3B. The simulation reproduces the experimental spectra with a high degree of accuracy with respect to the position of particular peaks on the field axis. Note that the $|2, -1\rangle \rightarrow |2, 0\rangle$ perpendicular signal that appears in the simulation at 10.6 T is obscured in the experiment by the $g = 2$ line at 10.4 T, which is from a Kramers spin impurity (see below). The accuracy with respect to peak amplitude and shape is also good. Some of the weaker simulated transitions originate from excited spin states such as $|2, -1\rangle$ and $|2, 0\rangle$. These *do* appear in the experimental spectrum at 8.4 and 11.7 T, which confirms the correctness of the chosen parameter set. Close inspection of the perpendicular $|2, -2\rangle \rightarrow |2, -1\rangle$ transition reveals that it is doubled (inset in Figure 3A). This doubling could be reproduced in the simulations by introducing a small rhombic parameter E equal to 0.015 cm^{-1} as shown in the same figure. The complete spin Hamiltonian parameters, including uncertainties, are given in Table 1. The uncertainties (± 0.01 both in g value and D (in cm^{-1})) arise mainly from the relatively large line width of the observed signals: single-crystal line widths used in the simulations were 100 mT for parallel transitions and 70 mT for perpendicular.

We have tried to obtain further information by raising the temperature, and populating the excited M_S states, as we did in the case of [Mn^{III}TPP(Cl)] and [Mn^{III}Pc(Cl)],[8] and as was done for [(tpfc)Mn(OPPh$_3$)] by Bendix et al.[10] However, this was not successful since the overall spectrum intensity rapidly decreased so that by 10 K no EPR spectrum was detectable. This is a notable difference from the above complexes, in which Mn(III) spectra could be observed at ~30 K, and may be attributed to the higher spin relaxation rates in **1** compared to the other complexes.

Pyridine Frozen Solution. Dissolution in air of **1** in pyridine affects its HFEPR spectra as shown in Figure 3C, recorded at 276.62 GHz and 4.2 K. The set of lines previously attributed to an $S = 2$ spin species persists in frozen solution although the signals shift noticeably. For example, the strong line observed in solid **1** at 14.6 T at 291 GHz shifts above the magnet field range (limited to 15 T at 4.2 K magnet coil temperature); however, lowering the microwave frequency to 276.6 GHz brings the line back within the range, to appear at 14.4 T. The corresponding parallel $|2, -2\rangle \rightarrow |2, -1\rangle$ transition shifts to lower field in frozen glass compared to the solid, at given operating frequency. The doubling of the perpendicular $|2, -2\rangle \rightarrow |2, -1\rangle$ transition becomes more pronounced than in the solid state and is also detectable in transitions originating from excited M_S states such as $|2, -1\rangle \rightarrow |2, 0\rangle$. Spectra were observable above 10 K, which means that the relaxation properties of complex **1** in pyridine frozen solution are different than in the solid state. The rather high nominal concentration of **1** in pyridine (0.2 M), necessitated by sensitivity requirements, may raise some doubts whether all solid was actually dissolved. The quality of the HFEPR spectra, their almost-perfect random pattern, and at the same time, the meaningful differences between the frozen solution and solid spectra all convince us that the dissolution was complete.

The entire frozen solution spectrum shown in Figure 3C can be readily simulated as shown in Figure 3D, using the spin Hamiltonian parameters given in Table 1. The single-crystal line widths used in the simulations are significantly smaller than those used in the simulations of the solid (50 mT, isotropic for the frozen solution vs 100 and 70 mT for parallel and perpendicular line width, respectively, of the solid), consistent with the full dissolution argument. Figure 5 shows the frozen solution spectrum recorded at 97.70 GHz, accompanied again by its simulation. A single set of spin Hamiltonian parameters reproduces with very good accuracy the experimental spectra at any frequency for $S = 2$. The "extra line" present at 2.2 T at

(18) Jacobsen, C. J. H.; Pedersen, E.; Villadsen, J.; Weihe, H. *Inorg. Chem.* **1993**, *32*, 1216−1221. The simulation software package is freely distributed by Dr. H. Weihe; for more information see the WWW page: http://sophus.kiku.dk/software/epr/epr.html.

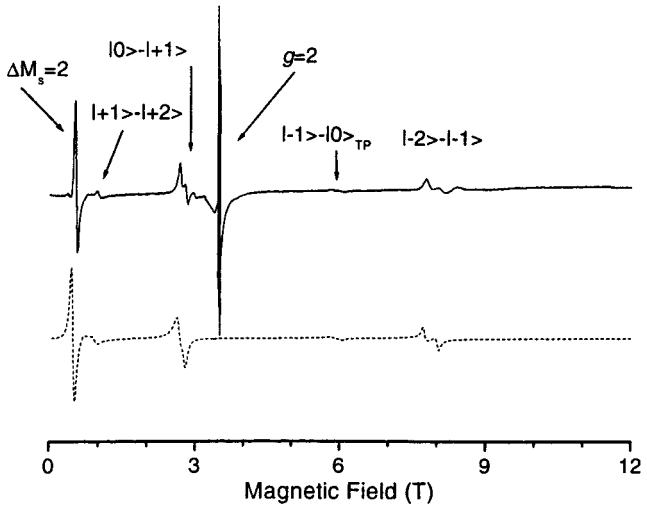

Figure 5. HFEPR spectrum of a frozen pyridine solution of complex **1** (solid line) and its simulation (broken line). Frequency 97.70 GHz, $T = 4.2$ K. Experimental parameters as in Figure 1, except for field sweep rate, and field modulation amplitude, which were reduced to 0.01 T/min and 0.5 mT, respectively, in the $g = 2$ spectral region. The spin Hamiltonian parameters used in simulation are given in Table 1. Only *x*, *y*-transitions in the powder pattern are present at this frequency, with the exception of the partly allowed ($\Delta M_S = 2$) transition. "TP" stands for an off-axis turning point.

291 GHz in the solid spectra is absent in the frozen solution, which further proves that it originates from an impurity.

The $g = 2$ Signal. This transition appears in solid **1** and indicates the existence of a Kramers species such as Mn(II) ($3d^5$). At higher frequencies (386 GHz, not shown) this signal consists of a partly resolved hyperfine sextet, as is typically seen for Mn(II). Although its amplitude is comparable to the transitions originating from the non-Kramers Mn(III) (Figure 3A), the Mn(II) signal is isotropic and hence its intensity after integration (not shown) is at least 2 orders of magnitude lower than that of the Mn(III). For the purpose of discussing the spin and oxidation states of the Mn(III) corrole complex of interest, **1**, the Mn(II) present in the solid sample is therefore a minor impurity. This observation and interpretation is quite common to Mn(III) complexes.[11]

The $g = 2$ signal became much more pronounced in frozen pyridine solution compared to the solid. The relative intensity of this transition with respect to the $S = 2$ lines strongly depends on the time elapsed between preparation and freezing of the solution. While preparing the sample for experiments presented in Figures 3C and 5, we kept that time at a minimum (~15 min). If the sample was allowed to sit overnight at room temperature, the $g = 2$ line became dominant in the spectrum, but the $S = 2$ spectrum was still detectable (Figure S1 in the Supporting Information). When studied in more detail under increased field resolution conditions, the $g = 2$ signal showed a fully resolved sextet with the characteristic[19] hyperfine coupling constant $a(^{55}\mathrm{Mn}) = 9.1 \pm 0.2$ mT at any frequency, although *g*-strain became apparent at high frequencies resulting in broadening of individual hyperfine components, as seen in Figure 6. Upon closer inspection, an unstructured and much broader signal was also revealed, which was more prominent at higher frequencies than at lower ones. Its intensity increased relative to the hyperfine sextet as a function of frequency so that it dominated the spectrum at 277 GHz. Its line width was ~0.12 T at 277 GHz.

(19) Brudvig, G. W. In *Advanced EPR*; Hoff, A. J., Ed.; Elsevier: Amsterdam, The Netherlands, 1989.

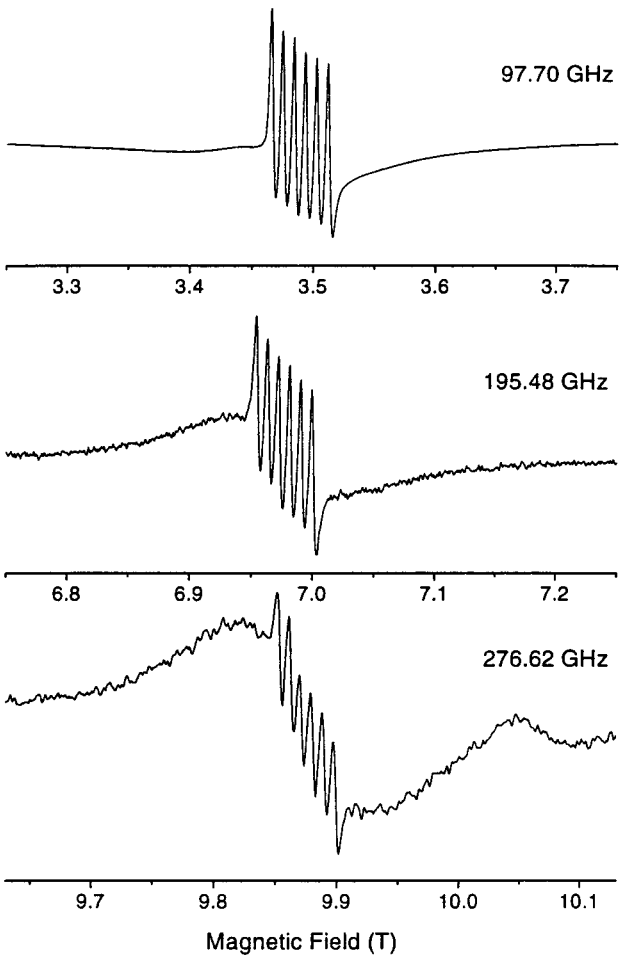

Figure 6. The $g = 2$ region of the frozen pyridine solution HFEPR spectrum of complex **1** at increased resolution at three different frequencies and $T = 4.2$ K. Experimental conditions as in Figure 1 except for the field sweep rate (0.01 T/min) and modulation amplitude (0.5 mT). The spectra are approximately normalized with respect to amplitude. The line at ca. 10.08 T at 277 GHz belongs to the $S = 2$ manifold.

X-band (at 77 K) and Q-band (35 GHz, at 4.2 K) EPR spectra of the aged pyridine solutions were also recorded (data not shown). The Q-band spectrum was recorded using electron spin−echo detection, which directly provides an absorption line shape.[17] Both types of spectra were characteristic of Mn(II). No signals were observed at $g > 2$.

Discussion

Complex 1 As a Solid. The HFEPR spectra of solid complex **1** can be unequivocally interpreted as arising from high-spin ($S = 2$) Mn(III) in a generally axial environment, making it "EPR-silent" at X-band. This conclusion was obtained earlier from XPS and magnetic susceptibility experiments on **1**.[13] A variety of other reports using HFEPR,[7,8,10] magnetic susceptibility,[20−23] and far-infrared spectroscopy[24] have all shown that solid-state Mn(III) porphyrinic[7,8,20−23] and corrole[10] complexes can best be described as $[\mathrm{Mn^{III}P^{2-}}]^+$ for porphyrins (including phthalo-

(20) Dugad, L. B.; Behere, D. V.; Marathe, V. R.; Mitra, S. *Chem. Phys. Lett.* **1984**, *104*, 353−356.
(21) Behere, D. V.; Mitra, S. *Inorg. Chem.* **1980**, *19*, 992−995.
(22) Kennedy, B. J.; Murray, K. S. *Inorg. Chem.* **1985**, *24*, 1557−1560.
(23) Goldberg, D. P.; Montalban, A. G.; White, A. J. P.; Williams, D. J.; Barrett, A. G. M.; Hoffman, B. M. *Inorg. Chem.* **1998**, *37*, 2873−2879.
(24) Brackett, G. C.; Richard, P. L.; Caughey, W. S. *J. Chem. Phys.* **1971**, *54*, 4383−4401.

cyanins and porphyrazines[7,8,23]) and as [$Mn^{III}C^{3-}$] for corroles.[10] We therefore begin by comparing and contrasting solid-state Mn(III) porphyrin and corrole complexes in terms of their chemical and electronic structure.

The crystal structure of **1** has not been solved to our best knowledge, but the structure of the very closely related complex, (7,13-dimethyl-2,3,8,12,17,18-hexaethylcorrolato)manganese-(III) (**2**), has been reported.[13] In **2**, the peripheral ring substitution is slightly more sterically demanding than in **1**, yet **2** is rigorously planar, making it unlikely that there are any distortions present in **1** that are absent in **2**. Furthermore, NMR studies performed on a series of manganese β-alkylcorrolates[13] and on the isoelectronic iron complexes[25] have shown that modifications on the pattern of β-alkyl substituents have no effect on the electronic structure of the coordinated metal ions. We will therefore assume that **1** and **2** are identical with respect to the Mn(III) environment and for simplicity refer to structural parameters for **1** that were actually determined for **2**. The structure of [(tpfc)Mn(OPPh$_3$)], investigated by HFEPR, has also been reported,[10] as have the structures of numerous Mn(III) porphyrinic complexes.[23,26,27]

In contrast to porphyrins, the direct link between pyrrole rings A and D (see Chart 1) found in corroles removes the 4-fold symmetry around the metal ion, so that the Mn−N(A,D) bond lengths are shorter (by ~0.01 Å) than for rings B and C, and the N(A)−Mn−N(D) bond angle is less than that for N(B)−Mn−N(C).[13] Given that the tetrapyrrole ligand defines the principal (z) axis as normal to the plane, such distortion of square-planar geometry would lead one to expect a rhombic (E) term ($x \neq y$) in the spin Hamiltonian. A nonzero rhombic term, $E = 0.015$ cm^{-1}, is indeed observed ($E/D = 0.006$), in contrast to the rigorously axial Mn(III) porphyrinic complexes.[7,8] Likewise, a somewhat larger rhombic term, $E = 0.030$ cm^{-1} ($E/D = 0.011$), was observed for [(tpfc)Mn(OPPh$_3$)].[10] However, the small relative and absolute magnitude of E led Bendix et al.[10] to suggest that Mn(III) corrole complexes are *electronically* nearly axial, despite the lower molecular symmetry, versus porphyrins. The current study on **1** provides a Mn(III) corrole that even more strongly supports their view. Clearly, the chemical differences between Mn(III) corroles versus porphyrins are not the consequence of macrocycle-imposed rhombic distortion about the metal ion.

Given that we can consider Mn(III) corroles to be roughly axial systems, we next compare the axial and equatorial ligand fields that exist in the complexes of interest. Corroles are trianionic tetrapyrrole ligands with smaller cores than in the dianionic porphyrins, with the result that the Mn−N bonds are shorter: 1.9 Å in corroles (1.894 Å in **1**[4] and 1.916 Å in [(tpfc)-Mn(OPPh$_3$)][10]) versus 2.0 Å for porphyrins.[1,4,13] Corroles can thus be considered to exert a stronger equatorial ligand field than do porphyrins.[1,4,13] In **1**, the Mn(III) ion is almost exactly in the ligand plane, while in the pentacoordinate complexes, the metal ion is displaced out-of-plane: by 0.26 Å in [MnTPP-(Cl)][26] and by 0.29 Å in [(tpfc)Mn(OPPh$_3$)].[10] As a result, complex **1** presumably has the strongest equatorial ligand field of the complexes of interest. Related to this, **1** has the weakest axial ligand field as it lacks an axial ligand, whereas the Mn-(III) corrole studied by Bendix et al. has an axial triphenylphosphane oxide ligand,[10] while Mn(III) porphyrins typically have axial halo, or other anionic, ligands.[7,8,20,22]

What is the relation between these structural and electronic effects and observed electronic parameters for these Mn(III) systems? Magnetic susceptibility and HFEPR studies of pentacoordinate Mn(III) porphyrins give $1.5 < |D| < 2.5$ cm^{-1}[7,8,20−22] with a negative sign of D unambiguously determined by HFEPR.[8] Bendix et al.[10] found for [(tpfc)Mn(OPPh$_3$)] $D = -2.69(2)$ cm^{-1},[28] while we find here for solid **1**, $D = -2.64(1)$ cm^{-1}. Referring to the discussion of Dugad et al.,[20] and to our previous work,[8] we see that the effect of the stronger equatorial ligand field for **1** compared to the other systems would be a larger value of Δ, the $d_{xy}-d_{x^2-y^2}$ separation. This would lead to a smaller magnitude D ($D \propto 1/\Delta$).[8] The effect of a weaker axial ligand field would be a larger value of δ_1, the $d_{xy}-d_{xz,yz}$ separation (ignoring the small rhombic splitting). This also would lead to a smaller magnitude D ($D \approx \lambda^2\{-4/\Delta + 1/(\Delta - \delta_1)\}$, $\Delta > \delta_1$).[8] Thus, if the contributions to axial zfs arose only from spin−orbit coupling among the spin quintet states, then D for **1** should be lower in magnitude (though still negative) than in the other systems. That **1** has a *larger* magnitude D than corresponding porphyrins means that there must be another contributing factor, such as that which we have previously defined[8] as $D' = -4\lambda^2/\delta_3$, where δ_3 is the energy separation between the spin quintet ground state ($d_{xy}^1 d_{xz,yz}^2 d_{z^2}^1$) and a spin triplet excited state ($d_{xy}^1 d_{xz,yz}^3$). For **1**, a smaller value for δ_3 more than compensates for the increases in Δ and δ_1 so that the total zfs has larger magnitude. It is unfortunately not possible to determine quantitatively the relative contributions of these two competing effects; however, it is interesting to note that **1** and [(tpfc)Mn(OPPh$_3$)] have almost the same magnitude of D. This might suggest an overall similarity among solid-state Mn-(III) corroles, despite differences in the axial ligand field and the relation of the Mn(III) ion to the corrole plane. The chief factor distinguishing Mn(III) corroles from porphyrins is that in corroles, the $S = 1$ excited state is significantly lower in energy. This may well be related to the relative instability of these complexes with respect to intramolecular redox processes in solution[1] and to their activity as oxidation catalysts.[6]

Complex 1 in Solution. We begin by noting that the present study is, to our knowledge, the *first* example of HFEPR detection of a non-Kramers system in nonaqueous frozen solution. However, the conclusions about the Mn oxidation and spin state of **1** in solution are not so clear-cut as they are for the solid-state complex. One of current authors' previous works[13] on manganese corroles in solution, based mostly on ambient temperature NMR and magnetic susceptibility experiments, postulated the formula [$Mn^{II}C^{\bullet 2-}$], with a total spin number of $S_{total} = 1$, as valid in the presence of coordinating solvents such as pyridine. The presence of an ion-radical localized on the corrole ring antiferromagnetically coupled to the metal ion was recognized by NMR for both iron and manganese complexes from the very large positive *meso*-proton shifts.[13,25] In these NMR studies, the *meso*-H shifts reported for the chloroiron corrolates[25] are much larger (170−190 ppm) than those of the Mn corrolates in pyridine solution (+70, +25 ppm),[13] suggesting that the antiferromagnetic coupling is much stronger in the [$Fe^{III}C^{\bullet 2-}$] than in the [$Mn^{II}C^{\bullet 2-}$] case. This implied that the Mn(II) ion must be intermediate-spin $S = {}^3/_2$, so that antiferromagnetic (AF) coupling yields the observed $S_{total} = {}^3/_2 - {}^1/_2 = 1$. This situation is analogous to that found by NMR for

(25) Cai, S.; Walker, F. A.; Licoccia, S. *Inorg. Chem.* **2000**, *37*, 2873−2879.

(26) Scheidt, W. R. In *The Porphyrins*; Dolphin, D., Ed.; Academic Press: New York, 1978. Scheidt, W. R.; Lee, Y. J. In *Metal Complexes with Tetrapyrrole Ligands*; Buchler, J. W., Ed.; Springer-Verlag: Berlin and Heidelberg, Germany, 1987.

(27) Boucher, L. J. In *Coordination Chemistry of Macrocyclic Compounds*; Melson, G. A., Ed.; Plenum: New York, 1979.

(28) In ref 10 the sign of D was left out, suggesting a positive value of D; however, this is a typographical error, as noted in a personal communication from J. Bendix. Our simulation of their reported temperature-dependent HFEPR unequivocally confirms that $D < 0$.

Mn porphyrins,[12] except for the character of magnetic coupling between the metal and the macrocycle radical, which was identified as ferromagnetic (FM) in the porphyrin complexes.

We would thus expect to detect a triplet spectrum in our HFEPR experiment in low-temperature pyridine glass, yet no signals that could be attributed to such a $S = 1$ system were identified; the spectrum was fully interpretable as a quintet ($S = 2$) state. This phenomenon may be due to the fact that NMR and magnetic susceptibility studies were performed on **1** at room temperature in fluid solution, while EPR spectra were detected in a low-temperature glass. It is thus conceivable that a temperature- and/or physical state-dependent change of electronic structure occurs for **1**.

There are, however, at least three scenarios by which this can occur. In one case (scenario A), the system is best described as an intermediate-spin Mn(II) ($S = {}^3/_2$) coupled to a ligand-centered radical, [$Mn^{II}C^{\bullet 2-}$], under all conditions, but the coupling changes from AF at ambient temperature, yielding $S_{total} = 1$ ($1 = {}^3/_2 - {}^1/_2$), to FM at low temperature, yielding $S_{total} = 2$ ($2 = {}^3/_2 + {}^1/_2$). Scenario B preserves the AF coupling between the metal ion and the radical under all conditions, but involves a change of the spin state of the Mn(II) ion from $S = {}^3/_2$ at room temperature to $S = {}^5/_2$ at low temperature. Both scenarios (and yet another one, involving Mn(IV)) are discussed by Kaustov et al.,[29] who also observed temperature-induced changes of total spin number in a chemically oxidized manganese porphyrin, [$Mn^{III}P^{\bullet -}]^{2+}$ from $S_{total} = {}^5/_2$ at 300 K to $S_{total} = {}^3/_2$ at 100 K. An alternative scenario C, which we are proposing here, depends on a temperature-dependent valence state isomerization: the complex is best described as [$Mn^{II}C^{\bullet 2-}$] at ambient temperature as in scenario A or B, but at low temperature, the system corresponds to [$Mn^{III}C^{3-}$], isolated Mn(III) with $S = 2$, as in the solid state.

Since EPR only indicates that the low-temperature system has $S_{total} = 2$, it cannot directly distinguish among the above scenarios. However, the zero-field splitting of complex **1** in pyridine frozen solution is very similar to that of the solid complex **1** (Table 1). The increase in $|D|$ and $|E|$ in low-temperature glass may be the result of axial pyridine coordination. Qualitatively, axial pyridine coordination would, in the converse of the process described before in the discussion of the solid complex, increase the axial ligand field, causing a decrease in δ_1, which leads to an overall *increase* in the magnitude of D, as observed (by ~10%). We have no specific explanation for the increase in E, except to note that **1** in solution exhibits rhombicity very close to that seen in solid [(tpfc)Mn(OPPh$_3$)], which might be a consequence of both complexes being pentacoordinate Mn(III) corroles, while solid **1** is tetracoordinate. Apparently the addition of these axial ligands reduces the axiality of the corrole ring system. Another interesting similarity between **1** in solution and solid [(tpfc)Mn(OPPh$_3$)] is that both exhibit HFEPR at temperatures >10 K, while solid **1** does not. In solid [(tpfc)Mn(OPPh$_3$)], there are no intermolecular interactions[10] (nor would these occur in frozen solution **1**), but these interactions are present in **1**.[13] As a result, spin relaxation from intermolecular exchange in solid **1** is much faster than in either **1** in frozen solution or in solid [(tpfc)Mn(OPPh$_3$)]. Other studies[30,31] carried out on copper and nickel corrolates point out that valence isomerization is favored by high temperature. We thus believe that this process, scenario C, is the case for **1** in pyridine solution.

The Origin of the $g = 2$ Signal. There remains the question about the origin of the $g = 2$ signal that is observable under any conditions, but becomes particularly prominent in aged pyridine solutions (Figures 6 and S1). It is quite obvious that this signal originates from a Kramers-type (half-integer) spin species, and that this species is either Mn(II) (usually $S = {}^5/_2$) or, less probably, Mn(IV) (usually $S = {}^3/_2$), as witnessed by the familiar hyperfine sextet characterized by the constant $a(^{55}Mn)$ of 9.1 mT. It is not, however, what would be expected for species derived from **1** in which the metal is the only paramagnetic center, namely [$Mn^{II}C^{3-}]^-$ or [$Mn^{IV}C^{3-}]^+$. Neither of the porphyrin analogues to these putative manganese corrole complexes give low-frequency ($h\nu \ll D$) EPR spectra consistent with that observed here using X- or Q-band EPR of aged pyridine solutions of **1**.[32] There is thus no clear correspondence between complex **1**, characterized by a variety of techniques, and the species yielding the $g = 2$ signal observed over time by EPR in pyridine solution stored at ambient temperature. Given the chemical activity of corroles relative to porphyrins,[1-3] it seems reasonable to conclude that this signal is due to a decomposition product as it does not resemble viable manganese tetrapyrrole species. Such decomposition, however, must involve only *minor* amounts of complex **1**, noting that all forms of EPR are very sensitive to detection of Kramers manganese ions, and that HFEPR is particularly apt at detecting minute quantities of Mn(II). More importantly, **1** is sufficiently stable in pyridine solution in air so that identical NMR spectra are recorded for fresh or aged (up to 24 h) pyridine solutions. A further proof of stability is that the monopyridine adduct of **1** and of manganese octaethylcorrolate can be recrystallized from pyridine/methanol without significant decomposition.[13] The exact nature of the $g = 2$ signal, and particularly the broad unstructured feature underlying the hyperfine sextet, remains beyond the scope of this work, but needs to be further investigated.

Conclusions

HFEPR of solid (8,12-diethyl-2,3,7,13,17,18-hexamethylcorrolato)manganese(III), **1**, shows that in the solid state it is well described as an $S = 2$ (high-spin) Mn(III) complex of a trianionic porphyrinic ligand, [$Mn^{III}C^{3-}$], just as Mn(III) porphyrins are described as [$Mn^{III}P^{2-}]^+$. Comparison among the structural data and spin Hamiltonian parameters reported for **1**,

(29) Kaustov, L.; Tal, M. E.; Shames, A. I.; Gross, Z. *Inorg. Chem.* **1997**, *36*, 3503−3511. In this study of a chemically oxidized Mn(III) porphyrin, the isolable solid, corresponding to [$Mn^{III}P^{\bullet -}]^{2+}$, exhibits X-band EPR spectra having strong, temperature-dependent signals at $g \approx 6$ and 4 characteristic respectively of $S = {}^5/_2$ or ${}^3/_2$ ground spin states in the case of $D > h\nu$. The authors offer three possible explanations for the observed phenomena: (A) the change of magnetic coupling character from ferromagnetic at room temperature to anti-ferromagnetic at low temperature; (B) the change of the Mn(III) oxidation state from high-spin $S = 2$ at room temperature to intermediate-spin $S = 1$ at low temperature, and (C) intramolecular oxidation of Mn(III) to Mn(IV). While no definite answer is given, case A is discarded as the least probable.

(30) Ghosh, A.; Wondimagegn, T.; Parusel, A. B. J. *J. Am. Chem. Soc.* **2000**, *122*, 5100−5104.

(31) Will, S.; Lex, J.; Vogel, E.; Schmickler, H.; Gisselbrecht, J.-P.; Hauptmann, C.; Bernard, M.; Gross, M. *Angew. Chem., Int. Ed. Engl.* **1997**, *36*, 357−361.

(32) Mn(II) porphyrins, [$Mn^{II}P^{2-}$], exhibit axial zfs characterized by $D \approx 0.5-0.7$ cm^{-1},[33] which yields X-band EPR spectra with signals near $g \approx 6$ for $S = {}^5/_2$, and should also be detectable at high-frequency conditions ($D \ll h\nu$). Corresponding Mn(IV) ($3d^3$) porphyrins, [$Mn^{IV}P^{2-}(X^-)_2$], exhibit X-band EPR spectra with signals near $g \approx 4$, as expected for $S = {}^3/_2$ with $h\nu \ll D$.[34] Neither X- nor Q-band EPR of aged pyridine solutions of **1** showed signals at these high g values, indicating the absence of [$Mn^{II}C^{3-}]^-$ or [$Mn^{IV}C^{3-}]^+$, and likely of [$Mn^{III}C^{\bullet 2-}]^+$, as well, by analogy with the porphyrin work by Kaustov et al.[29]

(33) Hori, H.; Ikeda-Saito, M.; Reed, G. H.; Yonetani, T. *J. Magn. Reson.* **1984**, *58*, 177−185.

(34) Camenzind, M. J.; Hollander, F. J.; Hill, C. L. *Inorg. Chem.* **1983**, *22*, 3776−3784.

Mn(III) porphyrins, and a different Mn(III) corrole, [(tpfc)Mn(OPPh$_3$)], previously studied by HFEPR,[10] shows that despite the molecular asymmetry of the corrole macrocycle, the electronic structure of the Mn(III) ion is roughly axial. However, in corroles the $S = 1$ (intermediate-spin) state is much lower in energy than in porphyrins, regardless of axial ligand. HFEPR of **1** in frozen pyridine solution shows that the $S = 2$ [$Mn^{III}C^{3-}$] system is maintained. This is in contrast to the room-temperature situation in which a $S = 1$ system was identified, deriving from antiferromagnetic coupling of the Mn(II) $S = {}^3/_2$ ion and a corrole-centered radical cation [$Mn^{II}C^{\bullet 2-}$]. This process has been explained by a temperature-assisted valence state isomerization. Over a period of hours in pyridine solution, an increasingly strong $g = 2$ signal arises, which is assigned to an as-yet unidentified manganese complex arising from a decomposition product of **1**.

Acknowledgment. The authors thank the following institutions for support: NHMFL (J.K. and L.C.B.), Roosevelt University (J.T.), NSF (B.M.H.), and MURS and CNR (S.L.). Dr. H. Weihe, Ørsted Institute, Copenhagen, Denmark, is kindly acknowledged for his simulation program and help in implementing it, and Ms. C. D'Ottavi is acknowledged for technical assistance. Professor D. Budil, Northeastern University, Boston is acknowledged for the software routine that allowed elimination of dispersion from the HFEPR spectra presented in Figure 1.

Supporting Information Available: HFEPR spectra of the pyridine solution of **1** as a function of the time spent between solution preparation and freezing (PDF). This material is available free of charge via the Internet at http://pubs.acs.org.

JA010947G